Journal of Computational Science 74 (2023) 102166

Contents lists available at ScienceDirect

Journal of Computational Science

journal homepage: www.elsevier.com/locate/jocs

An optimal homotopy continuation method: Convergence and visual analysis

Krzysztof Gdawiec [a,*], Ioannis K. Argyros [b], Sania Qureshi [c,d,e], Amanullah Soomro [c]

[a] Institute of Computer Science, University of Silesia, Bedzinska 39, Sosnowiec, 41-200, Poland
[b] Department of Computing and Mathematics Sciences, Cameron University, Lawton, OK 73505, USA
[c] Department of Basic Sciences and Related Studies, Mehran University of Engineering & Technology, Jamshoro, 76062, Pakistan
[d] Department of Mathematics, Near East University, Mersin, 99138, Turkey
[e] Department of Computer Science and Mathematics, Lebanese American University, Beirut, P.O. Box 13-5053, Lebanon

ARTICLE INFO

Keywords:
Fixed-point homotopy
Local convergence
Semi-local convergence
Basins of attraction
w-continuity condition

ABSTRACT

To avoid divergence in the traditional iterative root-finding methods the homotopy continuation approach is commonly used in the literature. However, neither their theoretical analysis in terms of local and semilocal convergence nor their stability is explored in the present literature. In this paper, we describe the homotopy continuation (HC) version of a fourth-order accurate optimal iterative algorithm. The local and semilocal convergence of the HC-based algorithm, including the basins of attraction, are being examined for the first time in the literature. These basins are used to demonstrate that the HC variant is more stable than the traditional iterative approach, which is widely held to be advantageous. The usual iterative method with first-order derivative is shown to be replaceable by its equivalent HC counterpart to achieve better stability for several numerical problems selected from academia and industry.

1. Introduction

Nonlinear equations, optimization problems, and eigenvalue problems are only some of the many scientific and technical challenges that can be solved with the help of the homotopy continuation approach. It is widely used in many fields, from physics and chemistry to biology and computer science [1,2]. Consider the following nonlinear equation:

$$f(x) = 0, \tag{1}$$

where f is a Fréchet-differentiable operator defined on a nonempty, open convex subset Ω of a Banach space B_1 with values in a Banach space B_2 [3,4]. Finding exact solution of (1) is not always possible because of nonlinearity and sometimes discontinuities in f. In such a case, researchers move to iterative algorithms for seeking approximate solutions to serve the purpose. One of the frequently used algorithms to find zeros of (1) is the second-order optimal Newton approach. However, there is a major drawback with Newton's method of finding the function's derivatives. If $f'(x)$ is more complicated to calculate than $f(x)$, then this could be a problem. Because of the divergence problem or slow convergence, Newton's method fails when $f'(x_0) = 0$. To avoid the inclusion of derivatives in algorithms, several researchers have developed new approaches [5–8]. For example, the secant method is a modified version of Newton's method that uses finite differences instead of derivatives to approximate the slope of the function f. It is a simpler and more stable method than Newton's approach, but it may converge more slowly. An algorithm called Brent's Method is a hybrid method that combines the bisection method, the secant method, and the inverse quadratic interpolation method. It is a highly efficient and robust method that can handle a wide range of functions, including highly nonlinear and discontinuous functions [9–11]. The Simultaneous Iteration Method is a powerful and versatile method for finding multiple roots of a set of nonlinear equations. It involves iterating a set of initial guesses, updating the guesses at each iteration using the equations, and checking for convergence to the roots. The method can handle highly nonlinear systems, but may converge slowly for complex systems. The Newton–Krylov Method is a powerful and efficient method for finding the roots of large systems of nonlinear equations. It combines the Newton–Raphson method with a Krylov subspace method to solve the linear systems that arise at each iteration [12]. The method is highly parallelizable and can handle large-scale problems with millions of unknowns [13]. Advanced root finding methods are powerful and versatile algorithms that can handle a wide range of functions, including highly nonlinear and discontinuous functions. Researchers and practitioners should choose the appropriate method based on the specific requirements of their problem, including accuracy, efficiency, robustness, and scalability.

* Corresponding author.
E-mail addresses: krzysztof.gdawiec@us.edu.pl (K. Gdawiec), ioannisa@cameron.edu (I.K. Argyros), sania.shahid@lau.edu.lb (S. Qureshi), amanullah.soomro@faculty.muet.edu.pk (A. Soomro).

https://doi.org/10.1016/j.jocs.2023.102166
Received 24 May 2023; Received in revised form 11 October 2023; Accepted 16 October 2023
Available online 18 October 2023

Moreover, the behavior of the iterative sequence close to the solution is the focus of local convergence. This means that our iterative procedure will converge to the correct solution if we begin "close enough" to the solution, as described in a recently published paper by Qureshi et al. [14]. Once convergence has started, it can move quickly with local convergence (as the quadratic convergence in Newton's method demonstrates). The problem is that it requires an approximate approximation to begin with, which is not always available. When compared to local convergence, semilocal convergence [15] is a more general term. In contrast to local convergence, it takes into account a larger domain around the solution and states that as long as the iterative process begins within this area, it will converge to the solution. When the relevant methods do not know the derivative (or second derivative) of the function, semilocal convergence might be very helpful [16]. The rate of convergence in some semilocally converging methods is not guaranteed to be as quick as in locally converging methods (like Newton's method), but these approaches can be more robust because the initial guess does not have to be extremely close to the actual solution. When solving nonlinear equations numerically, both local and semilocal convergences play important roles [17]. The quality of the initial guess, the availability of derivative information, and the nature of the problem all play a role in deciding which approach to choose. When applying numerical methods to solve real-world problems, knowing their convergence properties is essential since they shed light on the method's behavior and help choose the best approach.

In the light of above discussion, it can be observed that despite the existence of several powerful algorithms, there is always room to devise strategies that can either tackle the issue of divergence or/and reduce computational effort. In this case, the homotopy continuation method (HCM) provides a useful approach to finding the zeros of each function in terms of a convergent way to find the approximate solutions. Homotopy methods will convert a hard or complicated problem into a simpler one [18,19]. One of the main advantages of homotopy continuation iterative methods is their ability to find all solutions to nonlinear equations, including complex solutions, with a high degree of accuracy. Some other advantages of homotopy continuation iterative methods are the following:

- Robustness: Iterative approaches based on homotopy continuation are well-known for their sturdiness and dependability. They may deal with ill-conditioned problems and singular problems without encountering numerical difficulties.
- Efficiency: In many cases, iterative approaches based on homotopy continuation are more efficient than other existing methods at solving nonlinear equations.
- Flexibility: Iterative methods based on homotopy continuation are useful because they can be changed to solve a wide range of nonlinear equations, including ones with constraints, that depend on parameters, or that have unique structures.
- Convergence: Homotopy continuation iterative methods are guaranteed to converge to all the solutions of a nonlinear equation, regardless of the initial guess. This makes them particularly useful when there is no prior knowledge of the location of the solutions.

The present article is structured as follows. Section 2 presents some basic concepts related to the homotopy continuation method, while Section 3 shows the conversion of the optimal algorithm into its homotopy version. The local and semilocal convergence analysis for the optimal algorithm under consideration are discussed in Sections 4 and 5, respectively. Two numerical examples are solved in Section 6 to explain local and semilocal convergence. A detailed visual analysis via the polynomiography for the homotopy version of the algorithm is presented in Section 7. To prove the better performance of the homotopy continuation version, some numerical experiments including both academic and real-life situations are conducted in Section 8, whereas the concluding remarks with some future directions are described in Section 9.

2. Fundamentals of homotopy method

Homotopy continuation methods can be used to solve nonlinear equations. In fact, the method can be adapted to solve any kind of nonlinear equation, including polynomial and transcendental equations. The basic idea is still the same: to start with an easier-to-solve equation, and gradually transform it into the more difficult equation that one wants to solve. One popular choice for the homotopy function in this case is the so-called "power" or "homogeneous" homotopy. This homotopy involves adding a parameter to the equation, and defining a new equation that is a weighted sum of the original equation and a simple "homogeneous" equation. The weight of the original equation is gradually reduced as the parameter is varied, until the original equation is reached.

For example, suppose that we want to solve the nonlinear equation $f(x) = 0$. We can define a homotopy function Γ as:

$$\Gamma(x, \mu) = \mu f(x) - (1 - \mu)G(x), \tag{2}$$

where μ is a parameter that varies from 0 to 1, and G is an auxiliary function. For $\mu = 0$, we have $\Gamma(x, 0) = G(x)$, which is a simple equation with an easy solution. As μ increases, the weight of the original equation f increases, until at $\mu = 1$, we have $\Gamma(x, 1) = f(x)$, the equation we want to solve.

We can then use a numerical method, such as Newton's method or the secant method, to solve the simplified equation $\Gamma(x, 0)$, starting from an initial guess of the solution. As we gradually increase μ, we can track the solution of the original equation f by monitoring the solution path of the homotopy equation $\Gamma(x, \mu)$.

Homotopy continuation methods for solving nonlinear equations can be very effective, especially for equations that are difficult or impossible to solve analytically. However, like any numerical method, the success of the method depends on the choice of the homotopy function and the initial guess for the solution. To solve (1), one may define a homotopy or deformation function $\Gamma : \mathbb{R} \times \mathbb{R} \to \mathbb{R}$ such that

$$\Gamma(x, 0) = G(x), \qquad \Gamma(x, 1) = f(x), \tag{3}$$

where $\mu \in [0, 1]$ is the homotopy parameter and $G : \mathbb{R} \to \mathbb{R}$ is a user-defined, auxiliary function. G is usually defined to be similar to f, and the solution x_0 to $G(x) = 0$ is easier to determine. There are many types of auxiliary homotopy function [20], depending on G. For this study, the fixed-point function is selected as our auxiliary homotopy function since the function is simpler to use than others. In general, the fixed-point function is expressed as

$$G(x) = x_0 - x, \tag{4}$$

where x_0 refers to the initial guess. The most significant aspect of the auxiliary homotopy function is that this function must be controllable and uncomplicated to solve. As a final remark on the importance of homotopy methods, it can be observed that such methods based on homotopy ideas are not only used for nonlinear algebraic and transcendental equations but are equally applicable for solving differential equations [21–25].

3. Homotopy version for an optimal algorithm

In this section, we will attempt to convert an existing optimal fourth-order algorithm into its homotopy version with the help of the auxiliary homotopy function of the form $G(x) = x - x_0$. The considered optimal fourth-order algorithm was recently proposed in [26] as a linear combination of two iterative algorithms. The formula of the method is the following:

$$\begin{aligned} y_n &= x_n - \frac{f(x_n)}{f'(x_n)} \\ x_{n+1} &= x_n - \frac{f(x_n)\big(f(x_n)^2 - 3f(x_n)f(y_n) + f(y_n)^2\big)}{f'(x_n)\big(f(x_n) - 3f(y_n)\big)\big(f(x_n) - f(y_n)\big)}, \end{aligned} \tag{5}$$

where x_0 is the starting point.

The method given in (5), does not perform in the initial stage when $f'(x_0) = 0$ or $f'(x_0) \approx 0$ including two more possibilities as $f(x_n) - 3f(y_n) = 0$ or $f(x_n) - f(y_n) = 0$. To overcome this divergence problem, the following strategy based on fixed-point homotopy is presented:

$$\begin{aligned} y_n &= x_n - \frac{\Gamma(x_n,\mu)}{\Gamma'(x_n,\mu)} \\ x_{n+1} &= x_n \\ &\quad - \frac{\Gamma(x_n,\mu)\big(\Gamma(x_n,\mu)^2 - 3\Gamma(x_n,\mu)\Gamma(y_n,\mu) + \Gamma(y_n,\mu)^2\big)}{\Gamma'(x_n,\mu)\big(\Gamma(x_n,\mu) - 3\Gamma(y_n,\mu)\big)\big(\Gamma(x_n,\mu) - \Gamma(y_n,\mu)\big)}, \end{aligned} \tag{6}$$

where Γ is defined by (2). The above homotopy-based algorithm (6) is abbreviated as HCIA (Homotopy Continuation Iterative Algorithm) whose pseudo-code is presented in Algorithm 1.

Algorithm 1: Algorithm for HCIA

Input: $f : \mathbb{R} \to \mathbb{R}$ – function; x_0 – starting point; $G : \mathbb{R} \to \mathbb{R}$ – auxiliary function; $\varepsilon > 0$ – accuracy; N – the number of step for the homotopy; M – the number of iterations for the root-finding method.

Output: Root of f.

```
μ = 0
x = x_0
for i = 1, 2, ..., N do
    μ = μ + 1/N
    j = 0
    while j < M and |Γ(x, μ)| ≥ ε do
        j = j + 1
        y = x − Γ(x, μ)/Γ'(x, μ)
        x = x − Γ(x,μ)(Γ(x,μ)^2 − 3Γ(x,μ)Γ(y,μ) + Γ(y,μ)^2) / (Γ'(x,μ)(Γ(x,μ) − 3Γ(y,μ))(Γ(x,μ) − Γ(y,μ)))
return x
```

4. Local convergence analysis

If the results of Γ are to be trusted, the function must be differentiable at least five times. Consequently, if Γ is not at least five times differentiable, we do not know if the algorithm (6) converges to this conclusion. So, this result only works for solving equations that are constrained in this way. This results in a large number of unsolved equations. For example,

$$\Gamma(x) = \begin{cases} x^2 \log x^2 + 4x^5 - 4x^4, & \text{if } x \neq 0, \\ 0, & \text{if } x = 0. \end{cases} \tag{7}$$

Since

$$\Gamma'''(x) = 120 \log x^2 + 240x^2 - 96x \tag{8}$$

is not bounded on $[-1, 2]$. So, the analysis does not guarantee that (6) will converge. Also, keep in mind that the only derivative in (6) is Γ'. Thus, a local convergence result based on the method's derivatives needs to be established. This is the purpose of this section. The concept of w-continuity [27] shall be used (see the new convergence conditions (A_1)–(A_4) that follow).

Let $l_0 \geq 0$, $l \geq 0$ and $\lambda \in [0, 1)$ be given constants. Set $a = \frac{1}{1-\lambda}$, $L_0 = a\mu l_0$ and $L = a\mu l$. Define the function $\rho_1 : [0, \frac{1}{L_0}) \to \mathbb{R}$ by

$$\rho_1(t) = \frac{Lt}{2(1 - L_0 t)} - 1.$$

Notice that $r_1 = \frac{2}{2L_0 + L} < \frac{1}{L_0}$ for $L_0 \neq 0$, $L \neq 0$. $\rho_1(r_1) = 1$ and r_1 is the only solution of the equation $\rho_1(t) - 1 = 0$ in the interval $(0, \frac{1}{L_0})$.

Moreover, define the functions $P : [0, \frac{1}{L_0}) \to \mathbb{R}$ and $q : [0, \frac{1}{L_0}) \to \mathbb{R}$ by

$$\begin{aligned} P(t) &= a\left[\frac{\mu l}{2}t^2 + \mu\left(1 + \frac{l_0 Lt}{4(1 - L_0 t)}\right)\frac{Lt^2}{2(1 - L_0 t)}\right. \\ &\quad \left. + (1 - \mu)\left(1 + \frac{Lt}{2(1 - L_0 t)}\right)t\right], \end{aligned}$$

and

$$\begin{aligned} q(t) &= a\left[\frac{\mu l}{2}t^2 + 3\mu\left(1 + \frac{l_0 Lt}{4(1 - L_0 t)}\right)\frac{Lt^2}{2(1 - L_0 t)}\right. \\ &\quad \left. + (1 - \mu)\left(1 + \frac{3Lt}{2(1 - L_0 t)}\right)t\right]. \end{aligned}$$

By these definitions $P(0) - 1 = -1$, $q(0) - 1 = -1$ and $P(t) \to +\infty$, $q(t) \to +\infty$ as $t \to \frac{1}{L_0}$. Thus, the intermediate value theorem assures the existence of solutions for the equations $P(t) - 1 = 0$ and $q(t) - 1 = 0$ in the interval $(0, \frac{1}{L_0})$. Denote by ρ_p and ρ_q the smallest such solutions, and set $\rho = \min\{\rho_p, \rho_q\}$. Furthermore, define functions on the interval $[0, \rho)$ by

$$\begin{aligned} b(t) &= a\mu\left(1 + \frac{l_0}{2}t\right) + 3\mu\left(1 + \frac{l_0 Lt^2}{2(1 - L_0 t)}\right)\frac{Lt^2}{2(1 - L_0 t)} \\ &\quad + 2(1 - \mu)t + 3(1 - \mu)\left(1 + \frac{Lt}{2(1 - L_0 t)}\right)t, \\ c(t) &= a\left(\mu\left(1 + \frac{L_0}{2}t\right) + (1 - \mu)\right), \\ e(t) &= \frac{al}{2} + (1 + a\mu l_0 t)\mu\left(1 + \frac{l_0}{2}(1 + \frac{Lt}{2(1 - L_0 t)})t\right) \\ &\quad + (1 - \mu)\left(1 + \frac{Lt}{2(1 - L_0 t)}\right) \\ &\quad + a(1 + \mu l_0 t)(\mu(1 + \frac{l_0 Lt^2}{4(1 - L_0 t)}) + (1 - \mu))\frac{Lt}{2(1 - L_0 t)}, \\ d(t) &= \frac{al}{2}b(t)c(t) \\ &\quad + a\left(\mu\left(1 + \frac{l_0 Lt^2}{4(1 - L_0 t)}\right) + (1 - \mu)\right)\frac{Le(t)}{2(1 - L_0 t)}, \end{aligned}$$

and

$$\rho_2(t) = \frac{d(t)}{(1 - L_0 t)(1 - P(t))(1 - q(t))} - 1. \tag{9}$$

Then, again by these definitions, $\rho_2(0) = -1$ and $\rho_2(t) \to +\infty$ as $t \to \rho$. Denote by r the smallest solution of $\rho_2(t) = 0$ in the interval $(0, \rho)$.

The constant r is the radius of convergence for the method (6) (see Theorem 1). Finally, these definitions imply that

$$0 \leq L_0 t < 1, \tag{10}$$

$$0 \leq P(t) < 1, \tag{11}$$

$$0 \leq q(t) < 1, \tag{12}$$

$$0 \leq \rho_i(t) < 1 \quad i = 1, 2, \ldots. \tag{13}$$

A relationship is established between the developed functions and the constant r with the functions in algorithm (6).

Suppose

- (A_1) There exists $\kappa^* \in S \subset \mathbb{R}$ solving the equation $f(x) = 0$ such that $f'(\kappa^*) \neq 0$, and set $\lambda = (1 - \mu)|f'(\kappa^*)^{-1}(1 - f'(\kappa^*))|$.
- (A_2) $|f(\kappa^*)^{-1}(f'(y) - f(\kappa^*))| \leq l_0|y - \kappa^*|$ for each $y \in S$.
- (A_3) $|f(\kappa^*)^{-1}(f'(z) - f(y))| \leq l|z - y|$ for each $y, z \in S_0$.
- (A_4) $T[\kappa^*, r] \subset S$.

Theorem 1. *Under the conditions (A_1)–(A_4) the following holds for (6) provided that $x_0 \in T(\kappa^*, r) \setminus \{\kappa^*\}$:*

$$\{x_m\} \subset T(\kappa^*, r), \tag{14}$$

$$|y_m - \kappa^*| \leq \rho_1(|x_m - \kappa^*|)|x_m - \kappa^*| \leq |x_m - \kappa^*| < r, \tag{15}$$

$$|x_{m+1} - \kappa^*| \leq \rho_2(|x_m - \kappa^*|)|x_m - \kappa^*| \leq |x_m - \kappa^*|, \tag{16}$$

and

$$\lim_{n\to+\infty} x_m = \kappa^*. \tag{17}$$

Proof. The functions Γ and Γ' are related to f and f' through the conditions (A_1)–(A_4). By the choice of λ and the condition (A_2), we can write

$$\begin{aligned}\Gamma'(\kappa^*) - f'(\kappa^*) &= \mu f'(\kappa^*) + (1-\mu) - f'(\kappa^*)\\ &= (\mu-1)f'(\kappa^*) + (1-\mu)\\ &= (1-\mu)(1-f'(\kappa^*)),\end{aligned}$$

thus

$$|f'(\kappa^*)^{-1}(\Gamma'(\kappa^*) - f'(\kappa^*))| = \lambda < 1.$$

Consequently, $\Gamma'(\kappa^*) \neq 0$ by the Banach Lemma on invertible functions [28] and

$$|\Gamma'(\kappa^*)^{-1} f'(\kappa^*)| \leq \frac{1}{1-\lambda} = a. \tag{18}$$

Then, the iterate y_0 exists by the first substep of the algorithm (6) for $m = 0$. By the estimate

$$\begin{aligned}|\Gamma'(x_m)^{-1}(\Gamma'(x_m) - \Gamma'(\kappa^*))| &\leq a\mu l_0|x_0 - \kappa^*|\\ &= L_0|x_m - \kappa^*| < 1,\end{aligned}$$

$\Gamma'(x_m) \neq 0$ and

$$|\Gamma'(x_m)^{-1} - \Gamma'(\kappa^*)| \leq \frac{1}{1 - L_0|x_m - \kappa^*|}. \tag{19}$$

Moreover, from the first sub-step of the algorithm (6)

$$\begin{aligned}y_m - \kappa^* &= x_m - \kappa^* - \Gamma'(x_m)^{-1}\Gamma(x_m)\\ &= \int_0^1 \Gamma'(x_m)^{-1}(\Gamma'(\kappa^* + \theta(x_m - \kappa^*))d\theta\\ &\quad - \Gamma'(x_m))(x_m - \kappa^*)\\ |y_m - \kappa^*| &\leq |\Gamma'(x_m)^{-1}\Gamma(\kappa^*)| \int_0^1 \Gamma'(\kappa^*)^{-1}(\Gamma'(\kappa^*\\ &\quad + \theta(x_m - \kappa^*))d\theta - \Gamma'(x_m))(x_m - \kappa^*)|\\ &\leq \frac{L|x_m - \kappa^*|^2}{2(1 - L_0|x_m - x^*|)}\\ &= \rho_1(|x_m - \kappa^*|)|x_m - \kappa^*| \leq |x_m - \kappa^*| < r,\end{aligned} \tag{20}$$

since we used

$$\Gamma'(\kappa^* + \theta(x_m - x^*)) - \Gamma'(x_m) = \mu(f'(\kappa^* + \theta(x_m - \kappa^*)) - f'(x_m)),$$

so

$$\begin{aligned}|\Gamma'(\kappa^*)^{-1} f'(\kappa^*) \int_0^1 f'(\kappa^*)^{-1}\mu(f'(\kappa^* + \theta(x_m - \kappa^*))d\theta\\ - f'(x_m))(x_m - \kappa^*)| \leq \frac{a\mu l}{2}|x_m - \kappa^*|^2 = \frac{L}{2}|x_m - \kappa^*|^2.\end{aligned}$$

Next, we establish the existence of the iterate x_{m+1}. In order to achieve this, $\Gamma'(x_m) \neq 0$, $\Gamma(x_m) - \Gamma(y_m) \neq 0$ and $\Gamma(x_m) - 3\Gamma(y_m) \neq 0$.

We can write in turn that

$$\begin{aligned}&\Gamma(x_m) - \Gamma'(x_m)(x_m - \kappa^*) - \Gamma(y_m) + \Gamma'(\kappa^*)\\ &\quad = \mu f(x_m) - (1-\mu)(x_0 - x_m) - (\mu f'(x_m)\\ &\quad + (1-\mu)(x_m - \kappa^*)) - (\mu f(y_m) - (1-\mu)(x_0 - y_m))\\ &\quad + (1-\mu)(x_0 - y_m) - (1-\mu)(x_0 - \kappa^*)\\ &\quad = \mu(f(x_m) - f(\kappa^*) - f'(x_m)(x_m - \kappa^*))\\ &\quad - \mu(f(y_m) - f(\kappa^*)) - (1-\mu)(x_0 - \kappa^* + y_m - \kappa^*),\end{aligned} \tag{21}$$

so

$$\begin{aligned}&|\Gamma'(\kappa^*)^{-1} f'(\kappa^*) f'(\kappa^*)^{-1}(\Gamma(x_m) - \Gamma'(x_m)(x_m - \kappa^*)\\ &\quad - \Gamma(y_m))| \leq a\left[\mu\frac{l}{2}|x_m - \kappa^*| + \mu\right| \int_0^1 f'(\kappa^*\\ &\quad + \theta(y_m - \kappa^*))d\theta||y_m - \kappa^*|\\ &\quad + (1-\mu)(|x_0 - \kappa^*| + |y_m - \kappa^*|)\Bigg]\\ &\quad \leq a\left[\mu\frac{l}{2}|x_m - \kappa^*|^2 + \mu(1 + \frac{l_0}{2}|y_m - \kappa^*|)|y_m - \kappa^*|\right.\\ &\quad + \left.(1-\mu)(|x_0 - \kappa^*| + |y_m - \kappa^*|)\right] \leq P_m < 1,\end{aligned} \tag{22}$$

thus $\Gamma(x_m) - \Gamma(y_m) \neq 0$ and for $x_m \neq \kappa^*$

$$|(\Gamma(x_m) - \Gamma(y_m))^{-1}\Gamma'(\kappa^*)| \leq \frac{1}{|x_m - \kappa^*|(1 - P_m)}, \tag{23}$$

where we also used

$$\begin{aligned}|f'(\kappa^*)^{-1} \int_0^1 (f'(\kappa^* + \theta(x_m - \kappa^*))d\theta - f'(\kappa^*) + f'(\kappa^*))|\\ \leq 1 + \frac{l_0}{2}|x_m - \kappa^*|.\end{aligned}$$

As in (21)

$$\begin{aligned}&|\Gamma'(\kappa^*)^{-1}(\Gamma(x_k) - \Gamma'(x_m)(x_m - \kappa^*) - 3\Gamma(y_m))|\\ &\leq a\left[\frac{\mu l}{2}|x_m - \kappa^*|^2 + 3\mu(1 + \frac{l_0}{2}|y_m - \kappa^*|)|y_m - \kappa^*|\right.\\ &+ \left.\mu(|x_0 - \kappa^*| + 3|y_m - \kappa^*|)\right] \leq q_m < 1,\end{aligned} \tag{24}$$

hence $\Gamma(x_m) - 3\Gamma(y_m) \neq 0$ and

$$|(\Gamma(x_m) - 3\Gamma(y_m))^{-1}\Gamma'(\kappa^*)| \leq \frac{1}{(x_m - \kappa^*)(1 - q_m)}. \tag{25}$$

Therefore, the iterate x_{m+1} exists by the second sub step of the algorithm (6). Define the functions $M_m = M = \mu\int_0^1(\kappa^* + \theta(x_m - \kappa^*))d\theta - (1-\mu)$, then

$$\Gamma(x_m) = \Gamma(x_m) - \Gamma(\kappa^*) = M(x_m - \kappa^*). \tag{26}$$

Consequently, by the second sub step of the algorithm (6) and (25)

$$x_{m+1} - \kappa^* = \frac{N}{D}(x_m - \kappa^*), \tag{27}$$

where

$$\begin{aligned}D &= \Gamma'(x_m)(\Gamma(x_m) - \Gamma(y_m))(\Gamma(x_m) - 3\Gamma(y_m)),\\ N &= \Gamma'(x_m)(\Gamma(x_m) - 3\Gamma(y_m))\Gamma(x_m) - M(\Gamma(x_m)\\ &\quad - 3\Gamma(y_m))\Gamma(x_m) - \Gamma'(x_m)(\Gamma(x_m) - 3\Gamma(y_m))\Gamma(y_m)\\ &\quad - M\Gamma(y_m)^2 = (\Gamma'(x_m) - M)(\Gamma(x_m) - 3\Gamma(y_m))\Gamma(x_m)\\ &\quad - \Gamma(y_m)(M\Gamma(y_m) + \Gamma'(x_m)(\Gamma(x_m) - 3\Gamma(y_m))).\end{aligned} \tag{28}$$

An upper bound on $|D^{-1}|$ is given by (19),(23) and (25) as

$$\begin{aligned}|D^{-1}| \leq &\frac{1}{1 - L_0|x_m - \kappa^*|}\frac{1}{|x_m - \kappa^*|(1 - P_m)}\frac{1}{|x_m - \kappa^*|(1 - q_m)}\\ &\frac{1}{|x_m - \kappa^*|^2(1 - L_0|x_m - \kappa^*|)(1 - P_m)(1 - q_m)}.\end{aligned} \tag{29}$$

We also need an upper bound on $|N|$. This is achieved by finding upper bounds for each of the expressions that constitute (28) in turn:

$$\begin{aligned}\Gamma'(x_m) - M &= \mu(f'(x_m)\\ &\quad - \int_0^1 f'(\kappa^* + \theta(x_m - \kappa^*))d\theta),\\ |\Gamma'(\kappa^*)^{-1}(\Gamma'(x_m) - M)| &\leq \frac{a\mu l}{2}|x_m - \kappa^*|^2,\\ \Gamma(x_m) - 3\Gamma(y_m) &= \mu(f(x_m) - f(\kappa^*))\\ &\quad - 3\mu(f(y_m) - f(\kappa^*))\\ &\quad - (1-\mu)(x_0 - x_m)\\ &\quad + 3(1-\mu)(x_0 - y_m),\end{aligned} \tag{30}$$

$$
\begin{aligned}
&|\Gamma'(\kappa^*)^{-1}(\Gamma(x_m) - 3\Gamma(y_m))| \le a\mu(1 + \frac{l_0}{2}|x_m - \kappa^*|)\\
&\quad |x_m - \kappa^*| + 3\mu(1 + \frac{l_0}{2}|y_m - \kappa^*|)|y_m - \kappa^*|\\
&\quad + (1-\mu)(|x_m - \kappa^*| + |x_0 - \kappa^*|) + 3(1-\mu)\\
&\quad (|y_m - \kappa^*| + |x_0 - \kappa^*|) = b_m,
\end{aligned} \tag{31}
$$

$$
\Gamma(x_m) - \Gamma(\kappa^*) = M(x_m - \kappa^*), \tag{32}
$$

$$
\begin{aligned}
&|\Gamma'(\kappa^*)^{-1} M(x_m - \kappa^*)|\\
&\quad \le a\left[\mu(1 + \frac{l_0}{2}|x_m - \kappa^*|)|x_m - \kappa^*| + (1-\mu)\right]\\
&\quad = c_m|x_m - \kappa^*|,
\end{aligned} \tag{33}
$$

$$
\begin{aligned}
&\Gamma(y_m) - \Gamma(\kappa^*) = \mu(f(y_m) - f(\kappa^*)) - (1-\mu)(\kappa^* - y_m)\\
&|\Gamma'(\kappa^*)^{-1}\Gamma(y_m)| = |\Gamma(\kappa^*)^{-1}(\Gamma(y_m) - \Gamma(\kappa^*))|\\
&\quad \le a\left[\mu(1 + \frac{l_0}{2}|y_m - \kappa^*|) + (1-\mu)\right]\\
&\quad |y_m - \kappa^*|
\end{aligned} \tag{34}
$$

$$
\begin{aligned}
&M - \Gamma'(x_m) = \mu(\int_0^1 f'(\kappa^* + \theta(x_m - \kappa^*))d\theta - f'(x_m)),\\
&|\Gamma'(\kappa^*)^{-1}(M - \Gamma'(x_m))| \le \frac{a\mu l}{2}|x_m - \kappa^*|,
\end{aligned} \tag{35}
$$

$$
\begin{aligned}
&\Gamma'(x_k)(\Gamma(x_m) - \Gamma(y_m)) = \Gamma'(x_m)\\
&\quad \left[\mu\int_0^1 f'(y_m + \theta(x_m - y_m))d\theta + (1-\mu)\right](x_m - y_m)\\
&\quad |\Gamma'(\kappa^*)^{-1}\Gamma'(x_m)\Gamma'(\kappa^*)^{-1}(\Gamma(x_m) - \Gamma(y_m))|\\
&\quad \le a(1 + \mu l_0|x_m - \kappa^*|)\left(\mu(1 + \frac{l_0}{2}(|x_m - \kappa^*|\right.\\
&\quad \left. + |y_m - \kappa^*|)) + (1-\mu)\right)(|x_m - \kappa^*| + |y_m - \kappa^*|),
\end{aligned} \tag{36}
$$

$$
\begin{aligned}
&|\Gamma'(\kappa^*)^{-1}\Gamma'(x_k)\Gamma'(\kappa^*)\Gamma(y_k)|\\
&\quad \le (1 + a\mu l_0|x_m - \kappa^*|)a(\mu(1 + \frac{l_0}{2}|y_m - \kappa^*|)\\
&\quad + (1-\mu))|y_m - \kappa^*|.
\end{aligned} \tag{37}
$$

In view of (28) and summing up (30)–(37), we obtain in turn

$$
\begin{aligned}
|N| &\le \frac{al}{2}b_m c_m|x_m - \kappa^*|^3 + a(\mu(1 + \frac{l_0}{2}|y_m - \kappa^*|\\
&\quad + (1-\mu))|y_m - \kappa^*|) + a\mu\frac{l}{2}|x_m - \kappa^*|\\
&\quad + (1 + a\mu l_0|x_m - \kappa^*|)(1 + \frac{l_0}{2}(|x_m - \kappa^*|)\\
&\quad + |y_m - \kappa^*| + (1-\mu))(|x_m - \kappa^*| + |y_m - \kappa^*|)\\
&\quad + (1 + a\mu l_0|x_m - \kappa^*|)a\mu(1 + \frac{l_0}{2}|y_m - \kappa^*|\\
&\quad + (1-\mu))|y_m - \kappa^*| \le d_m|x_m - \kappa^*|^3.
\end{aligned} \tag{38}
$$

Hence by (6), (14), (29), and (38)

$$
|x_{m+1} - \kappa^*| \le \rho_2(|x_m - \kappa^*|)|x_m - \kappa^*| \le |x_m - \kappa^*| \le |x_m - \kappa^*|. \tag{39}
$$

Therefore, iterate $x_{m+1} \in T[\kappa^*, r)$ and assertions (14)–(17) hold. Then, from the estimate

$$
|x_{m+1} - \kappa^*| \le R|x_m - \kappa^*| < R, \tag{40}
$$

for $R = \rho_2(|x_m - \kappa^*|) \in [0,1)$, the iterate $x_{m+1} \in T(\kappa^*, r)$ and $\lim_{n\to\infty} x_m = \kappa^*$. □

The next result determines the uniqueness domain for κ^*.

Proposition 1. *Assume:*

(i) $\upsilon \in T[\kappa^*, \rho_1)$ *solves the equation* $f(x) = 0$ *for some* $\rho_1 > 0$.
(ii) The condition (A_2) *is verified on the interval* $T[\kappa^*, \rho_1)$.
(iii) There exists $\rho_2 \ge \rho_1$ *such that*

$$
\frac{l_0}{2}\rho_2 < 1. \tag{41}
$$

Set $S_1 = S \cap T[\kappa^*, \rho_2]$.

Then, κ^* *is the only solution of the equation* $f(x) = 0$ *in the domain* S_1.

Proof. Define the function $M_1 = \int_0^1 f'(\kappa^*(\upsilon - \kappa^*))d\theta$.

By *(ii)* and (41)

$$
\begin{aligned}
|f'(\kappa^*)^{-1}(M_1 - f'(\kappa^*))| &\le l_0\int_0^1 (\upsilon - \theta)|\upsilon - \kappa^*|d\theta\\
&= \frac{l_0}{2}\rho_2 < 1, \text{ thus } M_1 \ne 0.
\end{aligned}
$$

Consequently, that $\upsilon = \kappa^*$ is implied by

$$
\upsilon - \kappa^* = M_1^{-1}(f(\upsilon) - f(\kappa^*)) = M^{-1}(0) = 0,
$$

concluding that $\upsilon = \kappa^*$ □

Clearly, in Proposition 1, we can set $\rho_1 = r$ provided that all the conditions of Theorem 1 are validated.

5. Semilocal convergence

Convergence can also occur on a limited basis, between the levels of local and global, and this is known as semi-local convergence. When more initial guesses are needed to reach convergence than are required for local convergence, we say that a root-finding method has semi-local convergence. To rephrase, the basin of attraction for a semi-local convergence approach is larger than that of a local convergence method, but smaller than that of a global convergence method.

Semi-local convergence iterative root-finding methods are numerical techniques used to approximate the roots of a given function that have semi-local convergence properties. Such methods are particularly useful in situations where it is difficult to determine the exact location of the root(s) or where the function has multiple roots that are close together.

Overall, semi-local convergence iterative root-finding methods offer a useful balance between the efficiency of locally convergent methods and the robustness of globally convergent methods.

This analysis follows as the local one, essentially replacing κ^* by x_0 and by using the analogous conditions to (A_1)–(A_4) and majorizing sequences [1,29]. Let $h_0, \ge 0 \quad h \ge 0, \quad s \ge 0$, and $\kappa^* \in [0,1)$, $\bar{\lambda} = (1-\mu)|f'(x_0)^{-1}(1 - f'(x_0))|$ provided that $x_0 \in S$ satisfies $f'(x_0) \ne 0$. Set $\bar{a} = \frac{1}{1-\bar{\lambda}}$, $\Gamma_0 = \bar{a}\mu h_0$, and $\Gamma = \bar{a}\mu h$. Let us develop sequences $\{\alpha_m\}$, $\{\beta_m\}$ for $\alpha_0 = 0, \beta_0 = s$ as

$$
\begin{aligned}
r_m^1 &= \bar{a}\left[\mu(1 + h_0(\alpha_m + \frac{1}{2}(\beta_m - \alpha_m))) + 1 - \mu\right](\beta_m - \alpha_m),\\
r_m^2 &= \Gamma(\beta_m - \alpha_m)^2,\\
r_m^3 &= \bar{a}\Gamma(1 + \mu h_0\alpha_m)(\beta_m - \alpha_m)^3,\\
r_m &= \Gamma(r_m^1 + r_m^2 + r_m^3),\\
\alpha_{m+1} &= \beta_m + \frac{3r_m}{1 - \Gamma(\beta_m - \alpha_m)^2},\\
\delta_{m+1} &= \frac{\Gamma}{2}(\alpha_{m+1} - \alpha_m)^2 + \bar{a}(1 + \mu\alpha_m)(\alpha_{m+1} - \beta_m),\\
\beta_{m+1} &= \alpha_{m+1} + \frac{\delta_{m+1}}{1 - \Gamma_0\alpha_{m+1}}.
\end{aligned} \tag{42}
$$

The sequences $\{\alpha_m\}$, $\{\beta_m\}$ are majorizing for the algorithm (6) (see Theorem 2). However, first a convergence result is established for the sequences.

Lemma 1. *Under the conditions*

$$
\Gamma(\beta_m - \alpha_m) < 1, \quad \text{and} \quad \Gamma_0\alpha_{m+1} < 1, \tag{43}
$$

the sequences $\{\alpha_m\}$, $\{\beta_m\}$ *generated by the formulae* (42) *satisfy*

$$\alpha_m \le \beta_m \le \alpha_{m+1} < \frac{1}{\Gamma_0}, \tag{44}$$

and

$$\lim_{m\to+\infty} \alpha_m = \lim_{m\to+\infty} \beta_m = \beta^* \le \frac{1}{\Gamma_0}. \tag{45}$$

Proof. The formulae (42) and the condition (43) lead to the estimate (44) from which (45) also follows. □

The limit point β^* is unique as the least upper bound of these sequences. The semi-local conditions corresponding to the local are:

- $(\subset_1)$ There exists $x_0 \in S$ and $S \ge 0$ such that $f'(x_0) \ne 0$ and $\bar{a}\mu|f'(x_0)^{-1}f(x_0)| \le S$.
- $(\subset_2)$ $|f'(x_0)^{-1}(f'(v) - f'(x_0))| \le h_0|v - x_0|$ for some $h_0 \ge 0$ and each $x \in S$. Set $S_2 = S \cap T\left(x_0, \frac{1}{h_0}\right)$.
- $(\subset_3)$ $|f'(x_0)^{-1}(f'(v_2) - f'(v_1))| \le h|v_2 - v_1|$ for some $h \ge 0$ and each $v_1, v_2 \in S_2$.
- $(\subset_4)$ The conditions (43) hold.
- $(\subset_5)$ $T[x_0, \beta^*] \subset S$.

Theorem 2. *Under the conditions* $(\subset_1) - (\subset_5)$ *there exists* $\kappa^* \in T[x_0, \beta^*]$ *solving the equation* $\Gamma(\mu, x) = 0$ *and such that*

$$|y_m - x_m| \le \beta_m - \alpha_m, \tag{46}$$

$$|x_{m+1} - y_m| \le \alpha_{m+1} - \beta_m, \tag{47}$$

and

$$|\kappa^* - x_m| \le \beta^* - \alpha_m. \tag{48}$$

Proof. The first two assertions are shown using induction. Indeed, the condition $(\subset_1)$ and (42) give in turn

$$\begin{aligned}|\Gamma'(x_0)^{-1}\Gamma(x_0)| &\le |\Gamma'(x_0)^{-1}f'(x_0)||f'(x_0)^{-1}\Gamma(x_0)|\\ &\le \bar{a}\mu|f'(x_0)^{-1}f(x_0)| = S = \beta_0 - \alpha_0 < \beta^*,\end{aligned}$$

where we also used

$$\begin{aligned}|f'(x_0)^{-1}(\Gamma'(x_0) - f'(x_0))| &= (1-\mu)|f'(x_0)^{-1}(1 - f'(x_0))|\\ &= \lambda_0 < 1,\end{aligned}$$

so

$$|\Gamma'(x_0)^{-1}f'(x_0)| \le \frac{1}{1-\lambda_0} = \bar{a}.$$

Similarly, we have

$$|\Gamma'(x_m)^{-1}\Gamma'(x_0)| \le \frac{1}{1 - \bar{a}\mu h_0|x_m - x_0|} = \frac{1}{1 - \Gamma_0|x_m - x_0|}. \tag{49}$$

Hence, the assertion (46) holds if $m = 0$ and the iterate $y_0 \in T(x_0, \beta^*)$.

By substituting the value of x_m from the first to the second subset we obtain as in the local case

$$\begin{aligned}x_{m+1} - y_m &= \left[1 - \frac{\Gamma(x_m)^2 - 3\Gamma(x_m)\Gamma(y_m) + \Gamma(y_m)^2}{D_1}\right]\\ &\quad (y_m - x_m) = \frac{N_1}{D_1}(y_m - x_m),\end{aligned} \tag{50}$$

where

$$D_1 = (\Gamma(x_m) - 3\Gamma(y_m))(\Gamma(x_m) - \Gamma(y_m)),$$

and

$$\begin{aligned}N_1 &= (\Gamma(x_m) - 3\Gamma(y_m))(\Gamma(x_m) - \Gamma(y_m)) - (\Gamma(x_m)\\ &\quad - 3\Gamma(y_m))\Gamma(x_m) - \Gamma(x_m)\Gamma(y_m)^2\\ &= -\Gamma(y_m)\left[(\Gamma(x_m) - \Gamma(y_m)) + \Gamma(x_m)\Gamma(y_m) - 2\Gamma(y_m)\right].\end{aligned}$$

Next, first we find an upper bound on $\frac{1}{D_1}$ provided that $y_m \ne x_m$ and $D_1 \ne 0$.

We need the estimates

$$\begin{aligned}\Gamma(x_m) - \Gamma(y_m) + \Gamma'(x_m)(y_m - x_m) &= -\mu(f(y_m) - f(x_m)\\ &\quad - f'(x_m)(y_m - x_m)) - |\Gamma'(x_m)^{-1}(y_m - x_m)(\Gamma(x_m)\\ &\quad - \Gamma(y_m) + \Gamma'(y_m)(y_m - x_m))|\\ &\le \frac{\bar{a}\mu h}{|y_m - x_m|}|y_m - x_m|^2 = \Gamma|y_m - x_m|\\ &\le \Gamma(\beta_m - \alpha_m) < 1,\end{aligned} \tag{51}$$

thus

$$|(\Gamma(x_m) - \Gamma(y_m))^{-1}\Gamma'(x_0)| \le \frac{1}{|y_m - x_m|(1 - \Gamma(\beta_m - \alpha_m))}, \tag{52}$$

and similarly

$$\begin{aligned}&\Gamma(x_m) - 3\Gamma(y_m) + \Gamma'(x_m)(y_m - x_m)\\ &\quad = \Gamma(x_m) - \Gamma(y_m) + \Gamma'(x_m)(y_m - x_m) - 2\Gamma(y_m)\\ &\quad + 2\Gamma(x_m) + 2\Gamma'(x_m)(y_m - x_m)\\ &\quad = -3(\Gamma(y_m) - \Gamma(x_m) - \Gamma'(x_m)(y_m - x_m)),\end{aligned} \tag{53}$$

so

$$|(\Gamma(x_m) - 3\Gamma(y_m))^{-1}\Gamma(x_0)| \le \frac{3}{|y_m - x_m|(1 - \Gamma(\beta_m - \alpha_m))}, \tag{54}$$

and by (50)–(54)

$$|\frac{1}{D_1}| \le \frac{3}{|y_m - x_m|^2(1 - \Gamma(\beta_m - \alpha_m))^2}. \tag{55}$$

Moreover, we need the estimates

$$\begin{aligned}\Gamma(x_m) - \Gamma(y_m) &= -\left[\mu(f(y_m) - f(x_m)) + (1-\mu)(y_m - x_m)\right]\\ &= -\left[\mu\int_0^1 f'(x_m + \theta(y_m - x_m))d\theta + (1-\mu)\right]\\ &\quad (y_m - x_m),\end{aligned} \tag{56}$$

so

$$\begin{aligned}|\Gamma(x_0)^{-1}(\Gamma(y_m) - \Gamma(x_m))| &\le \bar{a}\left[\mu(1 + h_0(|x_m - x_0|\right.\\ &\quad \left. + \frac{1}{2}|y_m - x_m|)) + (1-\mu)\right]|y_m - x_m|\\ &\le \bar{a}(\mu(1 + h_0(\alpha_m + \frac{1}{2}(\beta_m - \alpha_m)))\\ &\quad + (1-\mu))|y_m - x_m|,\end{aligned} \tag{57}$$

thus

$$\begin{aligned}|\Gamma'(x_0)^{-1}\Gamma(y_m)| &\le \bar{a}\mu h|y_m - x_m|^2 = \Gamma|y_m - x_m|^2,\\ \Gamma(x_m) &= -\Gamma'(x_m)(y_m - x_m),\end{aligned} \tag{58}$$

hence

$$\begin{aligned}|\Gamma'(x_0)^{-1}\Gamma(x_m)| &\le \bar{a}(1 + \mu h_0|x_m - x_0|)|y_m - x_m|\\ &\le \bar{a}(1 + \mu h_0\alpha_m)|y_m - x_m|.\end{aligned} \tag{59}$$

Summing up (56)–(59) and using the definition of N_1, we get

$$|N_1| \le r_m|y_m - x_m|^2. \tag{60}$$

Therefore, by (42), (55) and (60)

$$|x_{m+1} - y_m| \le \frac{3r_m}{(1 - \Gamma(\beta_m - \alpha_m))^2} = \alpha_{m+1} - \beta_m, \tag{61}$$

and

$$\begin{aligned}|x_{m+1} - x_0| &\le |x_{m+1} - y_m| + |y_m - x_0|\\ &\le \alpha_{m+1} - \beta_m + \beta_m - \alpha_0 = \alpha_{m+1} < \beta^*,\end{aligned}$$

so the iterate $x_{n+1} \in T(x_0, \beta^*)$ and the assertion (50) holds.

Moreover, the first sub-step for $m+1$ replacing m gives in turn

$$\Gamma(x_{m+1}) = \Gamma(x_{m+1}) - \Gamma(x_m) - \Gamma'(x_m)(x_{m+1} - x_m),$$

thus

$$\begin{aligned}|\Gamma(x_0)^{-1}\Gamma(x_{m+1})| &\leq \frac{\bar{a}\mu h}{2}|x_{m+1}-x_m|^2+\bar{a}(1+\mu|x_m-x_0|)\\ |x_{m+1}-x_m| &\leq \frac{\Gamma}{2}(\alpha_{m+1}-\alpha_m)^2+\bar{a}(1+\mu\alpha_m)\\ &(\alpha_{m+1}-\beta_m),\end{aligned} \tag{62}$$

consequently by (61) and (62)

$$\begin{aligned}|y_{m+1}-x_{m+1}| &\leq |\Gamma'(x_{m+1})^{-1}\Gamma'(x_0)||\Gamma'(x_0)^{-1}\Gamma(x_{m+1})|\\ &\leq \frac{\delta_{m+1}}{1-\Gamma_0\alpha_{m+1}}=\beta_{m+1}-\alpha_{m+1},\end{aligned} \tag{63}$$

and

$$\begin{aligned}|y_{m+1}-x_0| &\leq |y_{m+1}-x_{m+1}|+|x_{m+1}-x_0|\leq \beta_{m+1}-\alpha_{m+1}\\ &+\alpha_{m+1}-\alpha_0=\beta_{m+1}<\beta^*.\end{aligned} \tag{64}$$

Therefore, the iterates $\{\alpha_m\},\{\beta_m\}\in T[x_0,\beta^*)$, and the induction for the assertions (46) and (47) is completed. But the sequence $\{\alpha_m\}$ is Cauchy as convergent.

Consequently, the sequence $\{x_m\}$ is also Cauchy. Hence, there exists $\kappa^*\in T[x_0,\beta^*]$ such that $\lim_{m\to\infty}x_m=\kappa^*$. By setting $n\to\infty$ in (62) and the continuity of the function Γ imply $\Gamma(\kappa^*)=0$.

Finally for $j=0,1,2,\ldots$, the estimate

$$|x_{m+j}-x_m|\leq \alpha_{m+j}-\alpha_m, \tag{65}$$

for $j\to+\infty$ implies (48). □

The uniqueness domain for the solution follows in the next result as in the local case.

Proposition 2. *Suppose*

(i) $\upsilon\in T[x_0,\rho_3)$ *solves the equation* $f(x)=0$ *for some* $\rho_3>0$.
(ii) *The condition* $(\subset_2)$ *holds in the ball* $T[x_0,\rho_3)$.
(iii) *There exists* $\rho_4\geq\rho_3$ *such that*

$$\frac{h_0}{2}(\rho_3+\rho_4)<1.$$

Set $S_3=S\cap T[x_0,\rho_4]$.

Then, υ *is the only solution of the equation* $f(x)=0$ *in the domain* S_3.

Proof. Let $\bar{\upsilon}\in S_3$ be such that $f(\bar{\upsilon})=0$. Consider the function $Q=\int_0^1 f'(\upsilon+\theta(\bar{\upsilon}-\upsilon))d\theta$.

By applying the conditions (ii) and (iii)

$$\begin{aligned}|f'(x_0)^{-1}(Q-f'(x_0))| &\leq h_0\int_0^1[(1-\theta)|\upsilon-x_0|\\ &+|\bar{\upsilon}-x_0|]d\theta\leq\frac{h_0}{2}(\rho_3+\rho_4)<1,\end{aligned}$$

leading to $Q\neq 0$, so $\bar{\upsilon}=x$. □

Remark 1.

(i) The number $\frac{1}{\Gamma_0}$ can replace β^* in the condition $(\subset_5)$.
(ii) If all conditions of Theorem 2 hold, set $\rho_3=\beta^*$ and $\upsilon=\kappa^*$.
(iii) if $\mu=1$ in the preceding results then, we obtain immediately the corresponding local and semi-local results for the method (5).

6. Numerical simulations for local and semi-local convergence

In this section, we solve some numerical problems to discuss the results for local and semi-local convergence.

Problem 1. Define function f on the interval $[-1,1]$ by

$$f(x)=\exp(x)-1. \tag{66}$$

Clearly, $\beta^*=0$ solves the equation $\Gamma(x)=0$. It follows that convergence conditions are validated provided $l_0=\exp(1)-1$ and $l=\exp(\frac{1}{l_0})$. Then using the formula (9), the radius is $r=0.46285$.

According to Rheinboldt [30] and Traub [31], the radius of convergence for the standard two-step Newton's method is given by $r_0=\frac{2}{3l_1}$ where l_1 is the Lipschitz constant on the interval $[-1,1]$ satisfying the condition (A_3). The value of l_1 satisfying (A_3) for $k^*=0$ is $l_1=e$. Then, $r_0=0.24<r$. Hence, a larger radius of convergence is obtained, leading to a wider choice of initial points to force convergence of the new method.

Problem 2. Let $d\in(0,1)$. Define the function f on interval $[d,2-d]$ by

$$f(x)=x^3-d. \tag{67}$$

Choose as an initial point $x_0=1$. Then, the Lipschitz constants are $h_0=3-d$, $h=2(1+\frac{1}{h_0})$, $\alpha_0=0$, $d=0.95$ and $\beta_0=s=\frac{1-d}{3}$.

Table 1 shows that the conditions (A_1)–(A_4) are validated. Hence, $\lim_{n\to+\infty}x_n=\sqrt[3]{0.95}$.

7. Visual analysis via polynomiography

Visual analysis of root-finding methods via polynomiography is a standard tool in modern analysis of the quality of the root-finding methods [32]. The term polynomiography was coined out by B. Kalantari and it is a combination of the word "polynomial" and the suffix "graphy". In polynomiography we generate images called polynomiographs that show various aspects of the root-finding method depending on the coloring method [33]. In this section, we use one of the method of polynomiography, that is the basins of attraction. Using these polynomiographs, we compare the root-finding method given by (5) with its homotopy continuation version presented in Algorithm 1.

To generate basins of attraction, we assign a distinct color to each root of the considered polynomial, and for the non-convergent points, we select one more color (usually black). Now, each point of the area A that we want to visualize is taken as the starting point for the root-finding method. If the method has converged, then we search for the closest root of the polynomial and the found one and use its color to color the starting point. In the case when the method has not converged to any of the roots, we color the starting point using the additional color. In basins of attraction, we can observe to which root the given root-finding method converges depending on the starting point.

In this section, we generated basins of attraction for three complex polynomials of various degrees:

- $p_2(z)=z^2+8z-9$ with roots: -9, 1,
- $p_3(z)=z^3-1$ with roots: 1, $-\frac{1}{2}+\frac{\sqrt{3}}{2}\mathbf{i}$, $-\frac{1}{2}-\frac{\sqrt{3}}{2}\mathbf{i}$,
- $p_4(z)=z^4-0.75z^2-0.25$ with roots: -1, 1, $-0.5\mathbf{i}$, $0.5\mathbf{i}$.

For p_3 and p_4, we generated images in the area $A=[-2,2]^2$, and for p_2 the area was set to $[-10,2]\times[-6,6]$. The other parameters in each case were the same, i.e., the auxiliary function $G(z)=z-z_0$, where z_0 is the starting point, the maximal number of performed iterations by the root-finding method was set to 30 iterations, the computations accuracy $\varepsilon=0.001$, and the image resolution was set to 800×800 pixels. For the homotopy continuation version, we used several values of the number of steps (the parameter N in Algorithm 1). The program for generating the basins of attraction was written in Mathematica 13.2.

We start with the basins of attraction for the p_2 polynomial that are presented in Fig. 1. For the original method (5) in Fig. 1(a), we see that the two basins are separated by a vertical line in $z=-4$, i.e., in the middle between the two roots of p_2. Now, when we use the homotopy continuation method for (5), the basins form different shapes. The shape depends on the number of steps N in the method. For $N=5$ (Fig. 1(b)), we can observe that the basin corresponding to the root 1 (red color) is much larger than the basin for -9 (yellow

Table 1
Sequence for Problem 2 with $d = 0.95$.

n	0	1	2	3	4	5
$\Gamma_0 \alpha_{m+1}$	0.00244	0.05106	0.10480	0.16269	0.22566	0.29532
$\Gamma(\beta_m - \alpha_m)$	0.00310	0.05827	0.06387	0.06832	0.07363	0.08046

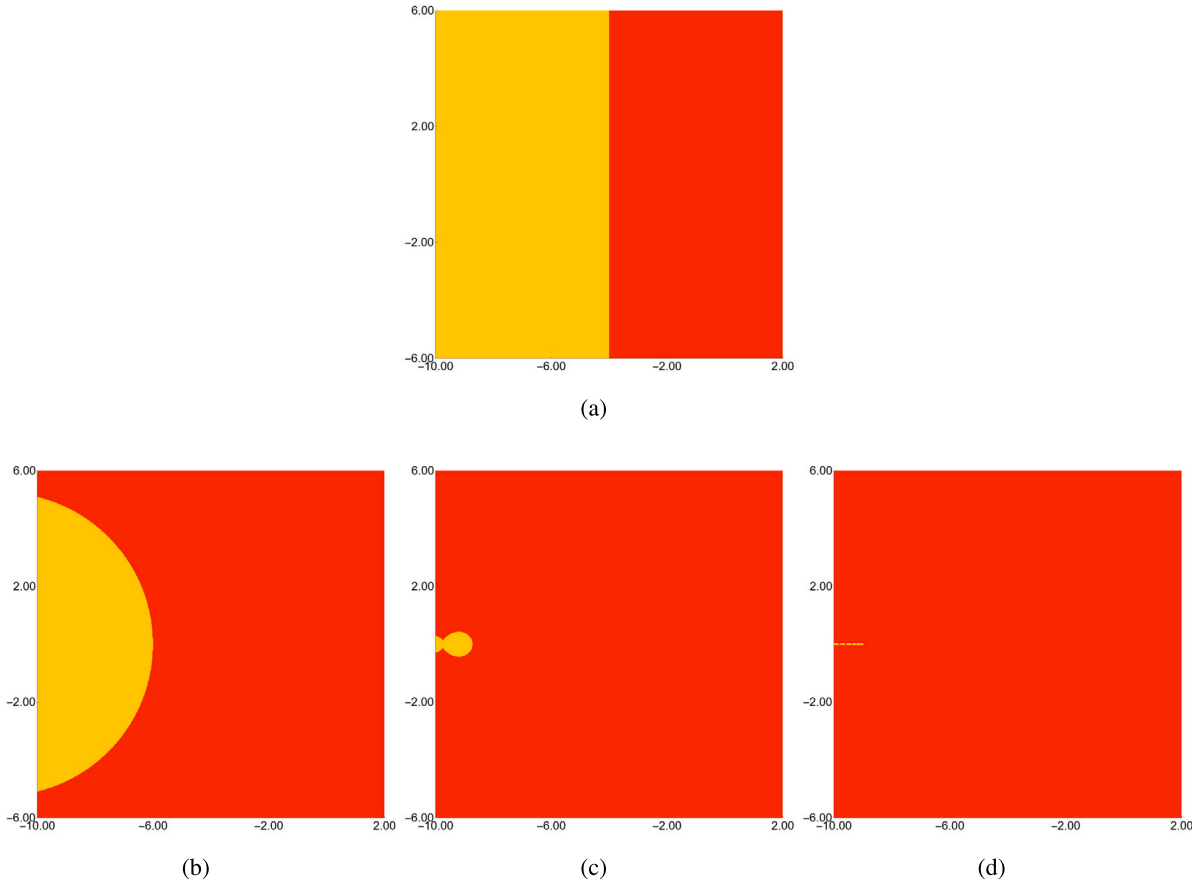

Fig. 1. Basins of attraction for the complex polynomial p_2 generated using (a) method (5), and its homotopy continuation version with various number of steps: (b) 5, (c) 20, (d) 100.

color). The boundary between these two basins is not a linear one, it is circular. When we increase N to 20 (Fig. 1(c)), then the yellow basin shrinks, and increasing N further to 100 (Fig. 1(d)) causes the yellow basin to almost disappear and the method converges only to the root 1.

In the next example, we visually analyze the basins of attraction (Fig. 2) for p_3. In the case of the original method (Fig. 2(a)), we can observe three characteristic braids that form the boundaries of the basins. Near these braids, the basins are interweaving each other, so the method do not works in a stable way. After using the homotopy continuation method the basins change their shape (Figs. 2(b)–(d)). For low values of N, i.e., $N = 5$ (Fig. 2(b)), we can observe that there are only two braids, and the interweaving is much smaller, which means that the stability of the method has increased. Moreover, the method mainly converges to the root associated with the yellow basin, i.e., to the real root 1. Next, for $N = 20$ (Fig. 2(c)), the boundaries of the basins are smoothed and they become more regular ones. There are some small areas near the boundaries in which we can observe the interweaving of the basins. Increasing the steps in the homotopy to 100 (Fig. 2(d)) smooths the boundaries further, obtaining clear boundaries between the three basins. Thus, the homotopy continuation method obtained better stability, than the original method given by (5).

In the last example, presented in Fig. 3, the basins of attraction for p_4 are analyzed. The basins for the original method (Fig. 3(a)) show very chaotic behavior. There are many interweavings between the basins, so the method does not work in a stable way. Now, when we use the homotopy continuation (Figs. 3(b)–(d)), then we notice an interesting behavior. No matter how many steps we use in the continuation, the basins are significantly different than the basins in Fig. 3(a). We do not see clear basins around the roots. Instead, we can observe that the basins remind us the ones that we saw in the case of the cubic polynomial p_3. For $N = 5$, we see some interweaving between the four basins, but considerably smaller than in the case of the original method. Moreover, we observe that the yellow basin that corresponds to the root -1 is very small. Then, when we increase the number of steps in the continuation to 20, the interweaving decreases, and the yellow basin almost disappeared. Increasing N to 100 smooths further the boundaries between the basins. The yellow basin reduces to isolated points scattered across the boundaries of the other three basins, mostly on the line that corresponds to the negative real line. From the images, we can also observe that the stability of the method that uses the homotopy continuation is better than the stability of the original method given by (5).

8. Numerical results for convergence analysis

We consider four nonlinear equations of scalar type. All examples use the homotopy function $\Gamma(x, \mu) = \mu f(x) + (1 - \mu)G(x)$. The auxiliary

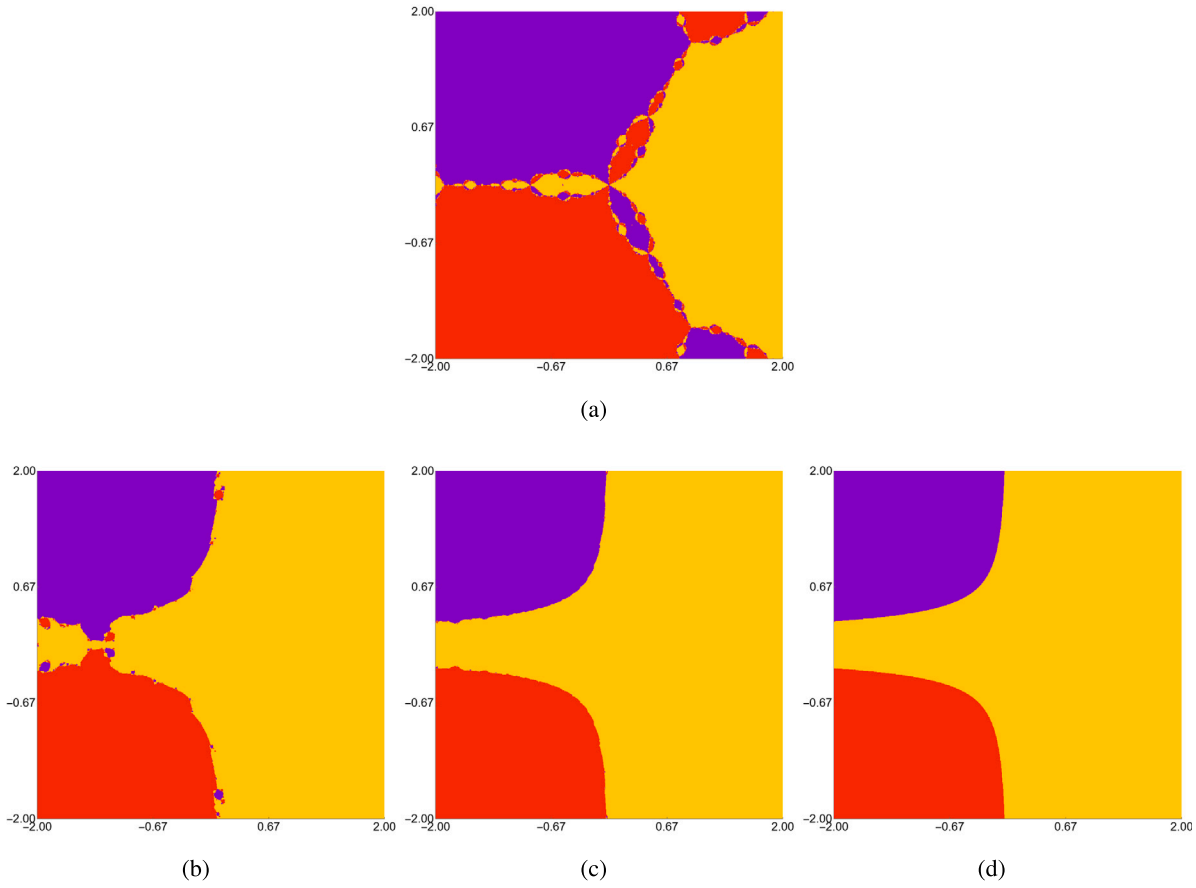

Fig. 2. Basins of attraction for the complex polynomial p_3 generated using (a) method (5), and its homotopy continuation version with various number of steps: (b) 5, (c) 20, (d) 100.

homotopy function G is taken to be $x - x_0$, where x_0 is the initial guess for the root of f. The stopping criterion is $|f(x)| < \varepsilon$ for the target function in the standard form of the method given in (5), while for its homotopy version given in (6), the stopping criterion is set to $|\Gamma(x,\mu)| < \varepsilon$, where $\varepsilon = 10^{-10}$. During simulations of the nonlinear equations via homotopy continuation method, the parameter $\mu \in [0,1]$ is taken in 10 steps.

8.1. Academic equations

Problem 3. Consider the following second-degree equation

$$f_1(x) = x^2 + 8x - 9. \tag{68}$$

f_1 has two real and distinct roots, namely 1 and −9 while its first-order derivative has a root −4 thereby causing the standard method (5) to fail at this point, including the points where $f(x) = 3f(x - \frac{f(x)}{f'(x)})$ or $f(x) = f(x - \frac{f(x)}{f'(x)})$. While the homotopy method given in (6) manages to reach the required roots. We saw polynomiographs for this function in Fig. 1. Table 2 shows a clear superiority of the homotopy continuation version over the standard optimal fourth-order method with different choices for the initial guess (x_0). Moreover, plot in Fig. 4(a) shows that the homotopy path is the function $x = x(\mu)$, where in every point $\Gamma(x,\mu) = 0$, while the plot in Fig. 4(b) shows that the HCM continuously deforms the known root of the start function G, into the root of the target function f_1.

Problem 4. Consider the following third-degree equation

$$f_2(x) = \frac{x^3}{3} - \frac{x^2}{2} - 6x + 1. \tag{69}$$

Table 2
Comparison of standard optimal fourth-order method with its homotopy continuation version while considering $G(x) = x - x_0$ for Problem 3.

x_0	Method (5)	Method (6)
−4	Diverge	1.00000000000029
−20	−9	1
1	Diverge	1
10	1	1
−9	Diverge	−9
−2	1.00000000000057	1.00000000000001

Table 3
Comparison of standard optimal fourth-order method with its homotopy continuation version while considering $G(x) = x - x_0$ for Problem 4.

x_0	Method (5)	Method (6)
−2	Diverge	−3.65270475885147
3	Diverge	4.98804937311281
0.05	0.164655385738718	0.164655385738718

The equation $f_2(x) = 0$ has three real and distinct roots: 4.98804937311281, 0.164655385738659 and −3.65270475885147, while its first-order derivative has two roots −2 and 3 thereby causing the standard method (5) to fail at these two points including the points where either $f(x) = 3f(x - \frac{f(x)}{f'(x)})$ or $f(x) = f(x - \frac{f(x)}{f'(x)})$. While the homotopy method given in (6) manages to reach the required roots. Table 3 shows a clear superiority of the homotopy continuation version over the standard optimal fourth-order method with different choices for the initial guess (x_0).

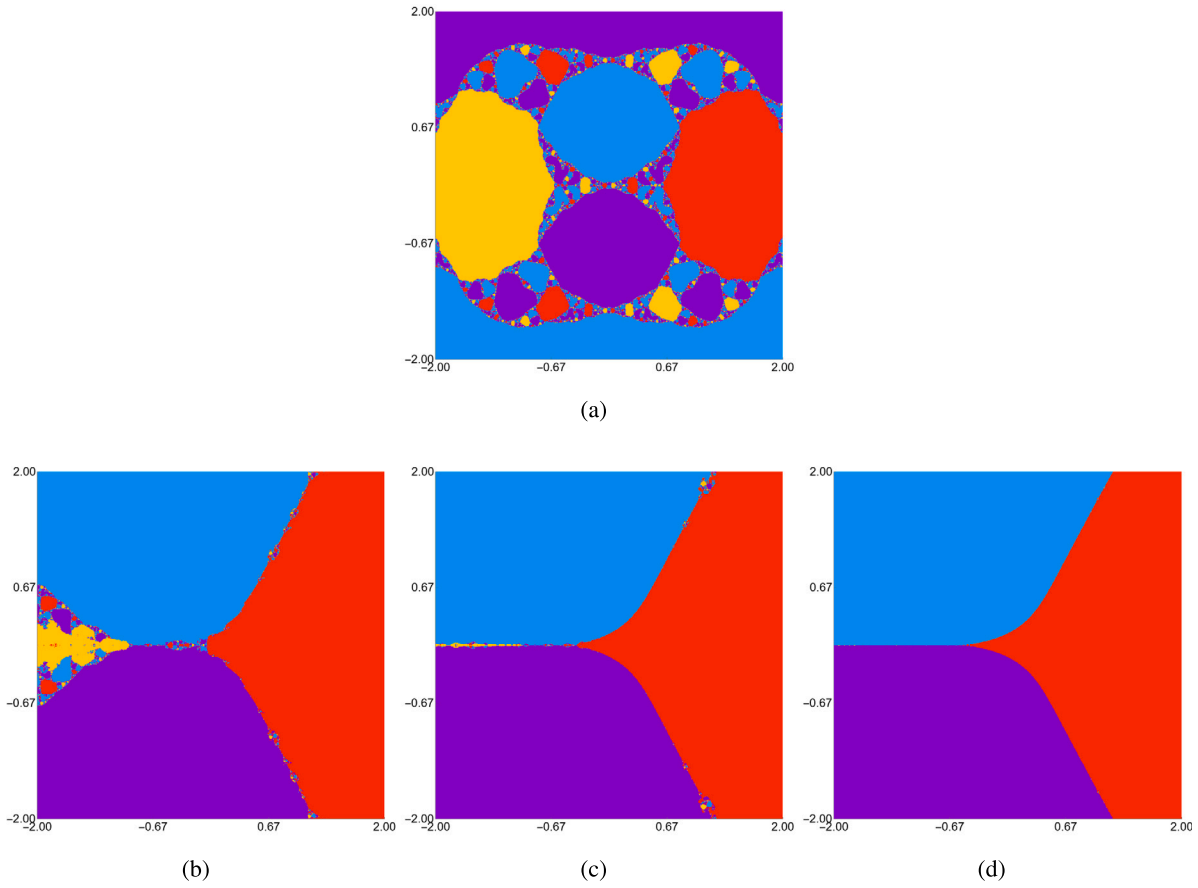

Fig. 3. Basins of attraction for the complex polynomial p_4 generated using (a) method (5), and its homotopy continuation version with various number of steps: (b) 5, (c) 20, (d) 100.

Table 4
Comparison of standard optimal fourth-order method with its homotopy continuation version while considering $G(x) = x - x_0$ for Problem 5.

x_0	Method (5)	Method (6)
−1.5	Diverge	−0.52228347176207
6.5	5.97508630942263	5.97508630941158
7.1	−0.522283471761962	5.97508630941158

Table 5
Comparison of standard optimal fourth-order method with its homotopy continuation version while considering $G(x) = x - x_0$ for Problem 6.

x_0	Method (5)	Method (6)
3.2943204	Diverge	5.89716695673287
2	0.691473843274813	5.89716695672519
10	5.89716695672600	5.89716695672519

Problem 5. A nonlinear equation involving some transcendental function is taken into consideration as follows [34]:

$$f_3(x) = \sin(x) - \frac{\cosh(x)}{1000} + 0.5. \tag{70}$$

The equation $f_3(x) = 0$ has some real roots in the interval $[-10, 10]$. The model in (70) has been simulated by methods (5) and (6) with the results shown in Table 4. From the results, it is easy to observe that the standard method (5) diverges for the initial guess $x_0 = -1.5$, while the homotopy method given in (6) manages to reach the required solution. In addition, the method without the homotopy continuation converges to the other solution with the initial guess $x_0 = 7.1$, whereas the homotopy continuation version does converge to the required solution. Table 4 shows a clear superiority of the homotopy continuation version over the standard optimal fourth-order method with different choices for the initial guess.

8.2. Real life applications

Problem 6. Consider the following azeotropic-point calculation discussed in Gritton et al. [35]

$$f_4(x) = x^2 - 6.5886408x + 4.0777367. \tag{71}$$

The function f_4 has two real and distinct roots namely $x_1 = 0.691473843274813$, $x_2 = 5.89716695672519$, while its first-order derivative has a root 3.2943204 thereby causing the standard method (5) to fail at this point including the points where either $f(x) = 3f(x - \frac{f(x)}{f'(x)})$ or $f(x) = f(x - \frac{f(x)}{f'(x)})$. While the homotopy method given in (6) manages to reach the required roots. Table 5 shows a clear superiority of the homotopy continuation version over the standard optimal fourth-order method with different choices for the initial guess (x_0). Even though the initial guess is chosen to be far away from the exact solution, the homotopy version manages to reach the desired root with much better accuracy in comparison to the standard method.

Problem 7 (*A model for uniform beam subject to a linearly increasing distributed load*)**.** [36] A typical nonlinear equation used to model beam positioning is the equation for the deflection of a beam under load. The deflection of a beam is affected by several factors, including the load applied, the shape of the beam, and the material properties of the beam. These factors interact in a non-linear way, resulting in a non-linear equation. One common form of the nonlinear equation used to model beam deflection is as follows:

$$f_5(x) = x^4 + 4x^3 - 24x^2 + 16x + 16, \tag{72}$$

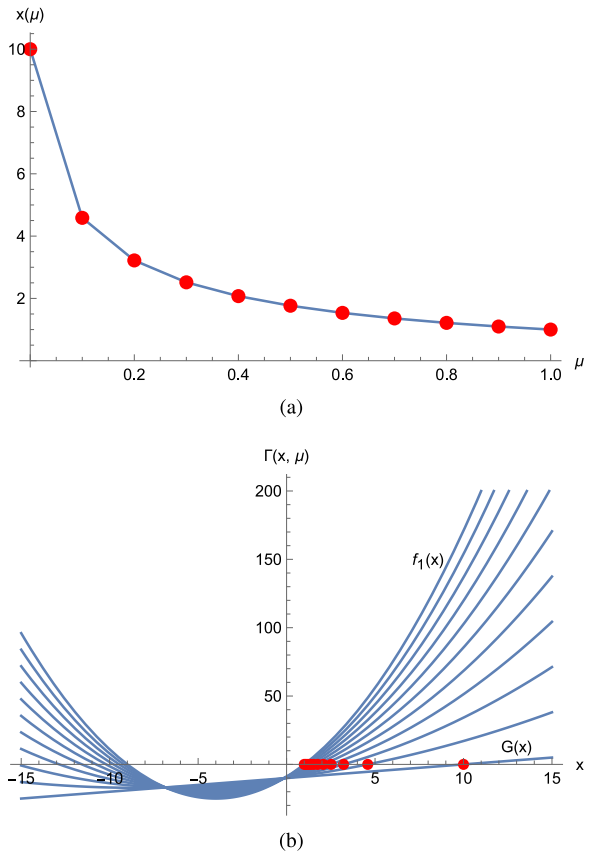

Fig. 4. (a) The homotopy path is the function $x = x(\mu)$, where in every point $\Gamma(x, \mu) = 0$. (b) Deformation of a root of the function $G(x) = x - x_0$ into a root of the polynomial $f_1(x) = x^2 + 8x - 9$ when $x_0 = 10$.

Table 6
Comparison of standard optimal fourth-order method with its homotopy continuation version while considering $G(x) = x - x_0$ for Problem 7.

x_0	Method (5)	Method (6)
0.5	Diverge	−7.46410161513775
0.3	−0.535898384862245	−0.535898384862245
5.0	Diverge	2.00000054065226

where x shows the maximum deflection.

The equation $f_5(x) = 0$ has four real roots, namely $x_1 = 2$, $x_2 = 2$, $x_3 = -7.4641016151378$, and $x_4 = -0.53589838486225$, while its first-order derivative has three distinct roots given as 2, 0.3722813232690143, and −5.372281323269014 thereby causing the standard method (5) to fail at these points including the points where $f(x) = 3f\left(x - \frac{f(x)}{f'(x)}\right)$ or $f(x) = f\left(x - \frac{f(x)}{f'(x)}\right)$. While the homotopy method given in (6) manages to reach the required roots. Table 6 shows a clear superiority of the homotopy continuation version over the standard optimal fourth-order method with different choices for the initial guess (x_0). Once again, the homotopy version of the standard method is observed to have the capability to yield all the required results.

9. Conclusions with future directions

In cases where the traditional approach does indeed diverge, the homotopy continuation variant of the optimal iterative algorithm with fourth-order precision has proven to converge. For the HC variant, we perform an analysis of local and semilocal convergence and provide some numerical examples. This development is a big deal in the world of numerical analysis and could be used in many other contexts. According to the findings of this research, the HC algorithm is both effective and efficient, and its further improvement is anticipated. The improved stability of the HC algorithm is demonstrated with the help of some polynomiographs.

As a whole, this work shows how crucial it is to find ways to optimize complex mathematical computations and how much room there is for future exploration and development in this area. More studies are needed to determine its utility in other contexts and to enhance its performance to its fullest potential. In addition, this algorithm may be able to be combined with other methods to form a more powerful and all-encompassing approach to solving a wide range of numerical analytic issues. Homotopy continuation methods are local methods, which means that they may converge to a local root or fail to converge at all. Homotopy continuation methods have applications in scientific computing, such as solving partial differential equations, control theory, and fluid dynamics. Developing methods that can efficiently solve these problems using homotopy continuation methods is an important research direction. Overall, the development of efficient and robust homotopy continuation methods and their applications to various fields is a promising research direction for the future.

Funding

The authors declare that no funds, grants, or other support were received during the preparation of this manuscript.

CRediT authorship contribution statement

Krzysztof Gdawiec: Conceptualization, Formal analysis, Investigation, Methodology, Software, Visualization, Writing – original draft, Writing – review & editing. **Ioannis K. Argyros:** Conceptualization, Validation, Writing – review & editing. **Sania Qureshi:** Conceptualization, Formal analysis, Methodology, Project administration, Software, Writing – original draft, Writing – review & editing. **Amanullah Soomro:** Formal analysis, Investigation, Writing – original draft, Writing– review & editing.

Declaration of competing interest

The authors declare that they have no known competing financial interests or personal relationships that could have appeared to influence the work reported in this paper.

Data availability

Data will be made available on request.

References

[1] I. Argyros, The Theory and Applications of Iteration Methods, second ed., CRC Press, Boca Raton, 2022, http://dx.doi.org/10.1201/9781003128915.
[2] R. Burden, J. Faires, A. Burden, Numerical Analysis, tenth ed., Cengage Learning Inc., Boston, 2015.
[3] I. Argyros, C. Argyros, J. John, J. Jayaraman, Semi-local convergence of two derivative-free methods of order six for solving equations under the same conditions, Foundations 2 (4) (2022) 1022–1030, http://dx.doi.org/10.3390/foundations2040068.
[4] S. Regmi, C. Argyros, I. Argyros, S. George, On the semi-local convergence of a Traub-type method for solving equations, Foundations 2 (1) (2022) 114–127, http://dx.doi.org/10.3390/foundations2010006.
[5] S. Qureshi, A. Soomro, A. Shaikh, E. Hincal, N. Gokbulut, A novel multistep iterative technique for models in medical sciences with complex dynamics, Comput. Math. Methods Med. 2022 (2022) 7656451, http://dx.doi.org/10.1155/2022/7656451.
[6] A. Tassaddiq, S. Quershi, A. Soomro, E. Hincal, D. Baleanu, A. Shaikh, A new three-step root-finding numerical method and its fractal global behavior, Fractal Fract. 5 (4) (2021) 204, http://dx.doi.org/10.3390/fractalfract5040204.

[7] I. Gosciniak, K. Gdawiec, One more look on visualization of operation of a root-finding algorithm, Soft Comput. 24 (18) (2020) 14135–14155, http://dx.doi.org/10.1007/s00500-020-04784-0.
[8] A. Naseem, M. Rehman, S. Quershi, N. Ide, Graphical and numerical study of a newly developed root-finding algorithm and its engineering applications, IEEE Access 11 (2023) 2375–2383, http://dx.doi.org/10.1109/ACCESS.2023.3234111.
[9] C. Sabharwal, An iterative hybrid algorithm for roots of non-linear equations, Eng 2 (1) (2021) 80–98, http://dx.doi.org/10.3390/eng2010007.
[10] M. Sarhan, An efficient approximate solution for non-linear solar cell equation using inverse quadratic interpolation method, J. Al-Qadisiyah Comput. Sci. Math. 12 (4) (2021) 49–54, http://dx.doi.org/10.29304/jqcm.2020.12.4.723.
[11] E. Badr, H. Attiya, A. Ghamry, Novel hybrid algorithms for root determining using advantages of open methods and bracketing methods, Alex. Eng. J. 61 (12) (2022) 11579–11588, http://dx.doi.org/10.1016/j.aej.2022.05.007.
[12] G. Formica, F. Milicchio, W. Lacarbonara, A Krylov accelerated Newton–Raphson scheme for efficient pseudo-arclength pathfollowing, Int. J. Non-Linear Mech. 145 (2022) 104116, http://dx.doi.org/10.1016/j.ijnonlinmec.2022.104116.
[13] N. Barnafi, L. Pavarino, S. Scacchi, Parallel inexact Newton–Krylov and quasi-Newton solvers for nonlinear elasticity, Comput. Methods Appl. Mech. Engrg. 400 (2022) 115557, http://dx.doi.org/10.1016/j.cma.2022.115557.
[14] S. Qureshi, I. Argyros, A. Soomro, K. Gdawiec, A. Shaikh, E. Hincal, A new optimal root-finding iterative algorithm: local and semilocal analysis with polynomiography, Numer. Algorithms (2023) 1–31, http://dx.doi.org/10.1007/s11075-023-01644-4 in press.
[15] C. Argyros, M. Argyros, I. Argyros, Á. Magreñán, Í. Sarría, Local and semi-local convergence for Chebyshev two point like methods with applications in different fields, J. Comput. Appl. Math. 426 (2023) 115072, http://dx.doi.org/10.1016/j.cam.2023.115072.
[16] J. Sharma, I. Argyros, H. Singh, Semilocal convergence analysis of an efficient Steffensen-type fourth order method, J. Anal. 31 (2) (2023) 1573–1586, http://dx.doi.org/10.1007/s41478-022-00538-3.
[17] S. Regmi, I. Argyros, S. George, C. Argyros, Extended semilocal convergence for Chebyshev–Halley-type schemes for solving nonlinear equations under weak conditions, Contemp. Math. 4 (1) (2023) 1–16.
[18] O. Axelsson, S. Sysala, Continuation Newton methods, Comput. Math. Appl. 70 (11) (2015) 2621–2637, http://dx.doi.org/10.1016/j.camwa.2015.07.024.
[19] J. Yakoubsohn, A universal constant for the convergence of Newton's method and an application to the classical homotopy method, Numer. Algorithms 9 (2) (1995) 223–244, http://dx.doi.org/10.1007/BF02141589.
[20] S. Rahimian, F. Jalali, J. Seader, R. White, A new homotopy for seeking all real roots of a nonlinear equation, Comput. Chem. Eng. 35 (3) (2011) 403–411, http://dx.doi.org/10.1016/j.compchemeng.2010.04.007.
[21] O. Bafakeeh, K. Al-Khaled, S. Khan, A. Abbasi, C. Ganteda, M. Khan, K. Guedri, S. Eldin, On the bioconvective aspect of viscoelastic micropolar nanofluid referring to variable thermal conductivity and thermo-diffusion characteristics, Bioengineering 10 (1) (2023) 73, http://dx.doi.org/10.3390/bioengineering10010073.
[22] Y. Jawarneh, H. Yasmin, M. Al-Sawalha, R. Shah, A. Khan, Numerical analysis of fractional heat transfer and porous media equations within Caputo–Fabrizio operator, AIMS Math. 8 (11) (2023) 26543–26560, http://dx.doi.org/10.3934/math.20231356.
[23] M. Nasir, M. Waqas, O. Bég, H. Ameen, N. Zamri, K. Guedri, S. Eldin, Analysis of nonlinear convection–radiation in chemically reactive oldroyd-B nanoliquid configured by a stretching surface with Robin conditions: Applications in nano-coating manufacturing, Micromachines 13 (12) (2022) 2196, http://dx.doi.org/10.3390/mi13122196.
[24] M. Partohaghighi, A. Akgül, E. Akgül, N. Attia, M. De la Sen, M. Bayram, Analysis of the fractional differential equations using two different methods, Symmetry 15 (1) (2022) 65, http://dx.doi.org/10.3390/sym15010065.
[25] M. Qayyum, E. Ahmad, H. Ahmad, B. Almohsen, New solutions of time-space fractional coupled Schrödinger systems, AIMS Math. 8 (11) (2023) 27033–27051, http://dx.doi.org/10.3934/math.20231383.
[26] S. Panday, A. Sharma, G. Thangkhenpau, Optimal fourth and eighth-order iterative methods for non-linear equations, J. Appl. Math. Comput. 69 (1) (2023) 953–971, http://dx.doi.org/10.1007/s12190-022-01775-2.
[27] J. Jaiswal, Semilocal convergence of a computationally efficient eighth-order method in Banach spaces under w-continuity condition, Iran. J. Sci. Technol. Trans. A Sci. 42 (2) (2018) 819–826, http://dx.doi.org/10.1007/s40995-016-0115-7.
[28] I. Argyros, Y. Cho, G. Santhosh, Local convergence for some third-order iterative methods under weak conditions, J. Korean Math. Soc. 53 (4) (2016) 781–793, http://dx.doi.org/10.4134/JKMS.j150244.
[29] I. Argyros, Unified convergence criteria for iterative Banach space valued methods with applications, Mathematics 9 (16) (2021) 1942, http://dx.doi.org/10.3390/math9161942.
[30] W. Rheinboldt, An adaptive continuation process for solving systems of nonlinear equations, Banach Center Publ. 3 (1) (1978) 129–142.
[31] J. Traub, Iterative Methods for the Solution of Equations, Prentice Hall, Inc., Englewood Cliffs, New Jersey, 1964.
[32] I. Petković, L. Rančić, Computational geometry as a tool for studying root-finding methods, Filomat 33 (4) (2019) 1019–1027, http://dx.doi.org/10.2298/FIL1904019P.
[33] B. Kalantari, Polynomial Root-Finding and Polynomiography, World Scientific, Singapore, 2009, http://dx.doi.org/10.1142/6265.
[34] S. Rahimian, F. Jalali, J. Seader, R. White, A new homotopy for seeking all real roots of a nonlinear equation, Comput. Chem. Eng. 35 (3) (2011) 403–411, http://dx.doi.org/10.1016/j.compchemeng.2010.04.007.
[35] K. Gritton, J. Seader, W.J. Lin, Global homotopy continuation procedures for seeking all roots of a nonlinear equation, Comput. Chem. Eng. 25 (7–8) (2001) 1003–1019, http://dx.doi.org/10.1016/S0098-1354(01)00675-5.
[36] A. Naseem, M. Rehman, T. Abdeljawad, Real-world applications of a newly designed root-finding algorithm and its polynomiography, IEEE Access 9 (2021) 160868–160877, http://dx.doi.org/10.1109/ACCESS.2021.3131498.

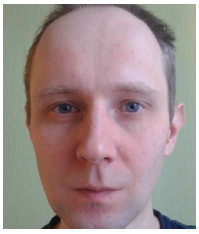

Krzysztof Gdawiec received his M.Sc. degree in mathematics from the University of Silesia (Poland) in 2005, the Ph.D. degree in computer science from the same university in 2010, and the DSc degree in computer science from the Warsaw University of Technology (Poland) in 2018. He is currently employed as an associate professor at the Institute of Computer Science of the University of Silesia. His main research interests include computer graphics, applications of fractal geometry, root-finding, game development, and the generation of Escher-like patterns. He is a member of the Polish Mathematical Society and SIGGRAPH.

Ioannis K. Argyros was born in Athens, Greece in 1956. In 1983, 1984 he received his M.Sc. and Ph.D., respectively in Mathematics from the University of Georgia, Athens, Georgia, USA. His area of expertise is Computational and Applied Mathematics in the wide sense. He has published over 1300 papers; 35 books and 21 chapters in books by others related to the aforementioned areas of research. He is also an editor in seventeen journals. His h-index is 42 and the number of citations is 10,120. He is currently a full professor at the Department of Computing and Mathematical Sciences at Cameron University.

Sania Qureshi was born in 1982 in Hyderabad, Pakistan. Qureshi earned her Ph.D. from the University of Sindh in 2019 and her postdoc from Near East University, Cyprus, in 2022. She visited the Division of Mathematics, University of Dundee, Scotland, UK, in 2016 and the Institute of Computational Mathematics, Technische Universitaet Braunschweig, Germany, in 2018 on two Ph.D. scholarships. Many of her publications are on mathematical epidemiology, fractional calculus, and numerical analysis. Qureshi has published over 100 Scopus and WoS research publications. Her current position is Associate Professor of Mathematics at Mehran University of Engineering and Technology in Jamshoro, Sindh.

Amanullah Soomro was born in Umerkot in 1995. In 2022, Mr. Soomro received his Master's degree from Mehran University of Engineering and Technology (MUET), Jamshoro, Sindh, Pakistan with Mathematics major. His area of expertise is Computational and Applied Mathematics. He is the co-author of 18 research papers recently published in Scopus international journals. Currently, Mr. Soomro is serving as a Lecturer at MUET.